Quaternary Research 74 (2010) 113–120

Contents lists available at ScienceDirect

Quaternary Research

journal homepage: www.elsevier.com/locate/yqres

Preliminary results from U–Th dating of glacial–interglacial deposition cycles in a silica speleothem from Venezuela

J. Lundberg [a,*], C. Brewer-Carias [b], D.A. McFarlane [c]

[a] Department of Geography and Environmental Studies, Carleton University, Ottawa, Ontario, Canada, K1S 5B6
[b] Sociedad Venezolana de Ciencias Naturales, Edif Torre America PH-B, Ave. Venezuela, Bello Monte Caracas, Venezuela
[c] W.M. Keck Science Center, The Claremont Colleges, Claremont, CA 91711, USA

ARTICLE INFO

Article history:
Received 7 August 2009
Available online 26 May 2010

Keywords:
Opal-A
Speleothem
U–Th date
Sandstone
Cave
Venezuela
Tepui
Glacial
Interglacial

ABSTRACT

Recent explorations in Cueva Charles Brewer, a large cave in a sandstone tepui, SE Venezuela, have revealed silica biospeleothems of unprecedented size and diversity. Study of one — a sub-spherical mass of opaline silica — reveals a complex, laminated internal structure consisting of three narrow dark bands alternating with two wider light bands. Uranium–thorium dating has produced 3 stratigraphically correct dates on the light bands from 298 ± 6 (MIS 9) to 390 ± 33 ka (MIS 11). U concentration is only 30–110 ppb. Initial $^{234}U/^{238}U$ ratios are high and increase over time from 1.8 to 5.3. Growth rate is very low, the fastest, at 0.37 ± 0.23 mm/ka, in MIS 9. Trace element and heavy metal content of the dark bands is distinctly higher than that of the light bands. It is hypothesized that the dark and light bands correlate with drier/glacial and wetter/interglacial periods, respectively, and that this sample probably began to grow in MIS 13. The cave is in a region that straddles a regionally important ecotone: the speleothem isotopic and trace element variations may preserve a useful paleoclimatic signal. This is the first published suite of U–Th dates from a single silica speleothem and the longest Quaternary record for this region.

Introduction

Cueva Charles Brewer, Venezuela, is developed at the top of Chimantá Plateau, a group of isolated tepuis in southeast Venezuela (Fig. 1). The tepuis are mesas or table mountains in Precambrian quartzites and sandstones. The cave hosts extraordinary silica speleothems that have been shown to be biologically mediated (Brewer-Carías, 2005; Aubrecht et al., 2008a). Silica speleothems have rarely been dated because they are usually very small in size and convoluted in form, and it is difficult to extract any useful information from them. Here we report the first suite of U–Th dates on these "biospeleothems" and, to our knowledge, the first suite of dates on a single silica speleothem.

Geographical and geological setting

Cueva Charles Brewer (Šmída et al., 2005) is developed within the uppermost 150–200 m of Churi-tepui. It functions as a major drainage system for much of the surface catchment. The tepuis are the western-most outliers of the Guiana Shield, formed largely of Precambrian silicate arenites of the Roraima Supergroup, ranging in age from 2.3 to 1.4 Ga (Piccini and Mecchia, 2009). The tepuis are developed mainly in the uppermost unit, the Mataui Formation, which has not been directly dated but can be presumed to be close to the minimum age of 1.66 ± 0.06 Ga (Gibbs and Barron, 1993) and certainly younger than 1.87 ± 0.03 Ga (Santos et al., 2003). Gibbs and Barron (1993) note that strictly they should be called "quasi-Roraima", being from a separate sedimentary basin; however, their characteristics are very similar. Gibbs and Barron (1993) describe the main mass of the Roraima Supergroup as a fairly mature quartz sandstone with a recrystallized matrix of sericitic quartzite, but with immature arkosic sandstones locally. They are relatively horizontal sedimentary rocks that have had only very low-grade burial metamorphism, and some local contact metamorphism from diabase intrusions (Piccini and Mecchia, 2009). The tepuis were uplifted 100 to 80 million years ago during the Late Cretaceous and subsequently dissected into separate table lands by erosion (Briceño and Schubert, 1990; Edmond et al., 1995; Potter, 1997).

As the largest known cave in sandstone or quartzite in the world, Cueva Charles Brewer is developed in one of the least lithified beds (Aubrecht et al., 2008b), paralleling the top of the tepui, and is currently at least 23 km long (unpublished data from 2009 expedition). Uniquely well-developed silica speleothems are found in many parts of the cave, generally out of the reach of flowing water, some reaching several tens of centimeters in diameter (see Brewer-Carías, 2005; Chacón et al., 2006; Aubrecht et al., 2008a).

* Corresponding author. Fax: +1 613 520 4301.
E-mail addresses: joyce_lundberg@carleton.ca (J. Lundberg), charlesbrewercarias@gmail.com (C. Brewer-Carias), dmcfarlane@jsd.claremont.edu (D.A. McFarlane).

0033-5894/$ – see front matter © 2010 University of Washington. Published by Elsevier Inc. All rights reserved.
doi:10.1016/j.yqres.2010.03.005

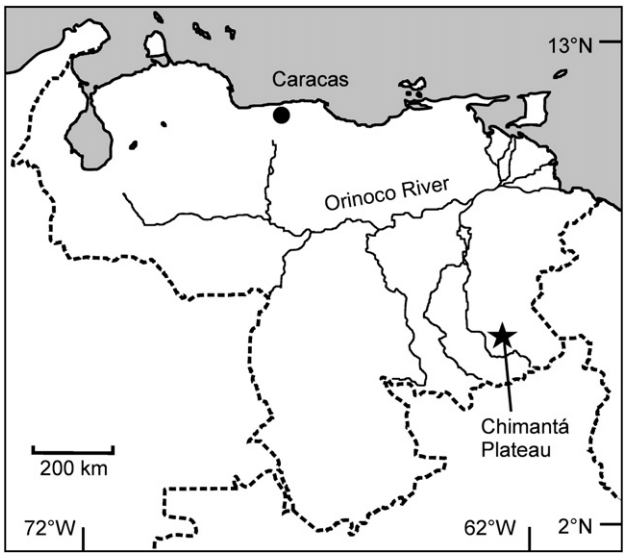

Figure 1. Location of Chimantá Plateau, Southeastern Venezuela.

Review of silica speleothems

The overwhelming majority of speleothems globally are formed as calcite because most speleothem-bearing caves have formed in carbonate rocks. Most silicate speleothems are reported from lava caves. Non-lava-hosted silicate speleothems are rare (Wray, 1999), and the few reports are generally in the gray literature. White et al. (1967) report the presence of banded opal coating the wall of a small fissure in Gran Sabana, Venezuela. A variety of silica speleothems including coralloid stalactites, stalagmites, and flowstone have been described by Hill and Forti (1997). Wray (1999) describes small, inorganically precipitated opal and chalcedony deposits on underhangs from Australia, of popcorn and coralloid form. Willems et al. (2002) report tiny coralloid speleothem made of opal and taranakite in a granitic cave of South Cameroon. Urbani et al. (2005) report opal crusts and coralloids up to 4 cm thick in the strongly evaporative entrance zone of a cave in a tepui in the Brazil–Venezuela border region. Twidale and Romani (2005), pages 251–255, after a brief review of the small siliceous stalactitic forms and thin coatings that develop in fissures of granite rocks, suggest that the speleothemic opal is precipitated biogenically in three stages. The first stage is precipitation of porous, brecciated, or oolitic silica from drying out of silica gel. The second stage is of direct biogenic precipitation by bacteria or fungi, along with internal re-solution causing progressive infilling of the porous material and, eventually, accretion at the surface in sequential laminae. The third stage is overgrowth by gypsum or other minerals. Cueva Charles Brewer has formed in sandstone/quartzite, so this setting is ideal for deposition of silica-rich speleothems.

The speleothems of Cueva Charles Brewer appear to be rather more complex than these small forms described from elsewhere. These speleothems are unique in that they stand in quasi-negative geotropic position but they are growing very obviously independently of any dripping water source and thus cannot be described by any of the 'normal' speleothem terms (such as stalagmites, stalactites, or helictites). This is why a whole suite of new terms has been created to describe them. Brewer-Carías (2005) and Aubrecht et al. (2008a,b) document in some detail the varieties. These include (i) mushroom-like forms of peloidal stromatolitic fabric (the "dolls"); (ii) black, intricately branched coralloid forms; (iii) ball-shaped "champignons" frequently more than 30 cm in diameter; (iv) compact, laminated, opalline forms (the "kidney"); and (v) the "cobweb" forms, partly abiotic siliceous encrustation of spiders threads. Regardless of shape, they all appear to consist of only two materials: (a) columnar stromatolitic material of nonporous compact opal, forming mostly the internal zones of the speleothems, the associated filaments identified as probable cyanobacteria; and (b) porous material of microbial peloids formed of white chalk-like opal, arranged in concentric laminae, forming mostly the outer zones of the speleothems. In some speleothems, both zones may alternate. All the speleothem of Cueva Charles Brewer are opal-A. Recrystallization to micro-quartz occurs in some speleothems but only in the older inner parts. For this study, we focused on one of the kidney forms.

The use of the term "biospeleothem" by Chacón et al. (2006) and Aubrecht et al. (2008a,b) indicates the basic premise that all are biologically mediated and that biological material has been found in all that were studied. The mechanism of formation has not been fully worked out yet, but they do appear to be strongly, if not completely, dependent on biological activity supplied by wicking of condensation waters through the speleothem bodies to the microbial mats on the surfaces and/or supply of water and nutrients from aerosols created by nearby waterfalls. Aubrecht et al. (2008a) have called them "large microbialites", a modification of the term first introduced by Burne and Moore (1987) to mean "organosedimentary deposits that have accreted as a result of a benthic microbial community trapping and binding detrital sediment and/or forming the locus of mineral precipitation". As with any speleothem study, the mode of formation has implications for paleoenvironmental reconstruction and, in turn, paleoenvironmental conditions may influence mode of formation.

Aim of study

Regardless of the mode of formation, the laminated nature implies sequential growth, which in turn implies the possibility of a paleoenvironmental record. This study uses U–Th dating as a test of the potential for paleoenvironmental reconstruction, to see if these samples can be dated and are within the ~600 ka range of the method, and to see if the growth is in fact sequential. For this study, one of the kidney types was studied, a part of the same specimen shown in Aubrecht et al. (2008a), Fig. 6C. The sample (Fig. 2) was collected in 2005 near Cascada Vanessa (Fig. 3), some 1–2 m above the highest flood level.

Methods

The sample was cut into several slices. The slab studied here (Fig. 4) is ~17 mm from core to edge. The sequence from core to outside edge is layer 1—the gray central core; layer 2—brown–black vuggy material; layer 3—pink silica; layer 4—black vuggy material; layer 5—pale cream silica with some orange tinted laminations (this is the 'pale peloidal zone' of Aubrecht et al., 2008a); layer 6—the outside thin dark layer. The left hand side shows remnants of a few additional, but no longer complete, younger layers.

U–Th dating

Three samples were taken from layers 3 and 5 (Fig. 4) for TIMS dating by standard U–Th disequilibrium techniques (e.g., Ivanovich et al., 1992). Material was drilled under binocular microscope, avoiding the colored laminations and the vuggy dark-colored material, and ultrasonically cleaned. All chemical preparation was done in ultraclean conditions. Samples were spiked with ^{233}U–^{236}U–^{229}Th tracer, dissolved in a mixture of concentrated HNO_3 and HF over 48 h on a hot plate, dried, and then taken up in 7 N HNO_3. U and Th were isolated on anion exchange columns (Dowex AG1-X 200-400 mesh). Measurement of U and Th isotopic ratios was made by thermal ionization mass spectrometry (TIMS) using the Triton thermal ionization mass spectrometer at the Isotope Geochemistry and Geochronology Research Facility, Carleton University, Ottawa,

https://doi.org/10.1016/j.yqres.2010.03.005 Published online by Cambridge University Press

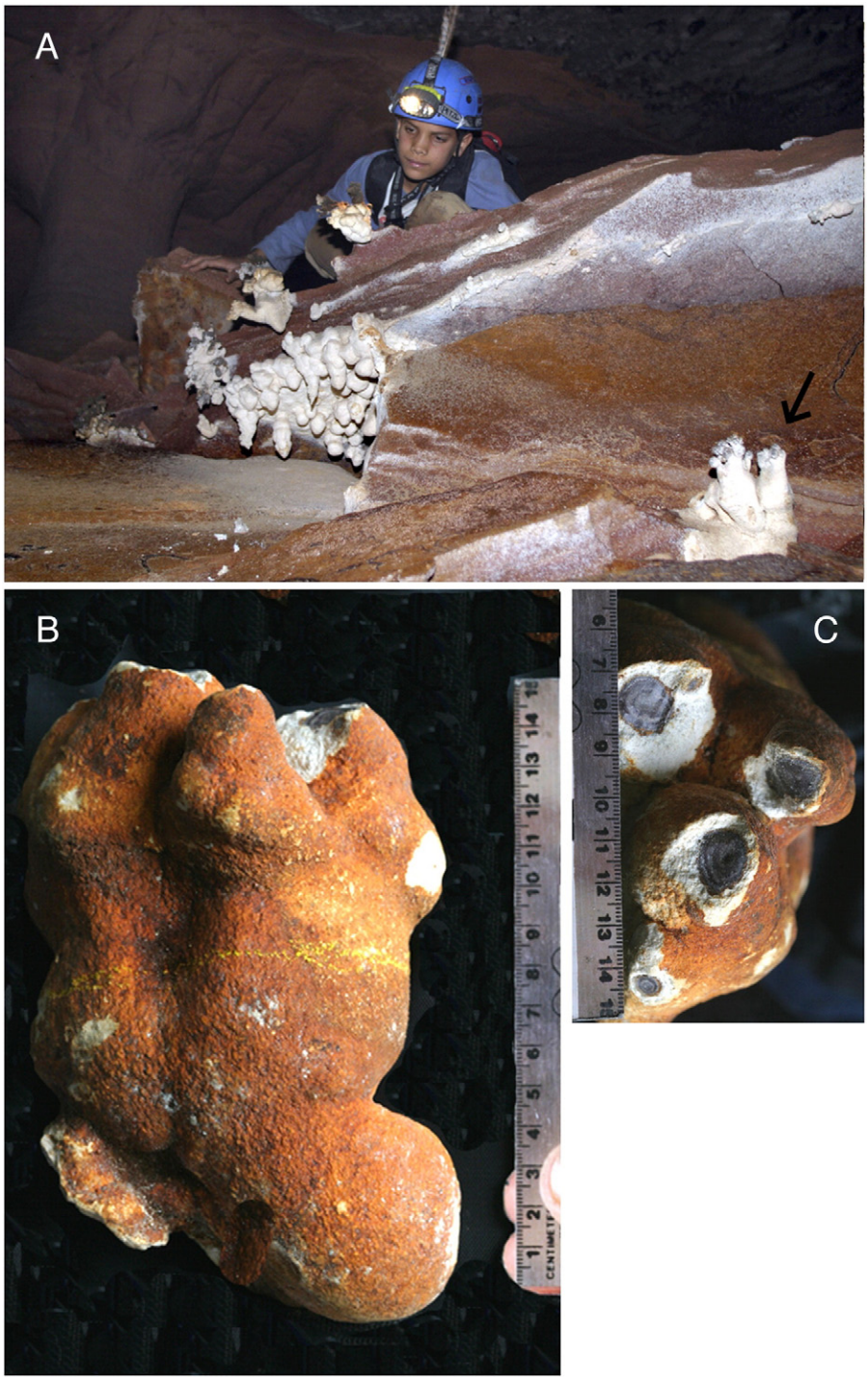

Figure 2. (A) The collection site for the sample (marked with black arrow), showing the typical growth habit on the edge of a block. (B) The entire sample before cutting, showing the small point of attachment on the bottom left and the nodular form. (C) Detail of the broken top showing the internal core and layered structure.

Ontario. The analyses were accompanied by the processing of uraninite in secular equilibrium to ensure accurate spike calibration and fractionation correction. Activity ratios were calculated using half lives from Cheng et al. (2000).

Although no sample showed visible detrital contamination on dissolution, the high ^{232}Th suggests some detrital contamination. Ages were adjusted for detrital contamination using the typical silicate activity ratio ^{230}Th/^{232}Th of 0.83 ± 0.42, derived from ^{232}Th/^{238}U activity ratio of 1.21 ± 0.6, ^{230}Th/^{238}U activity ratio of 1.0 ± 0.1, and ^{234}U/^{238}U activity ratio of 1.0 ± 0.1 (see Cruz et al., 2005). In all cases, the adjusted ages are within error of the raw ages.

X-ray diffraction and ICP-MS analysis

X-ray diffraction (XRD) from this sample has already been published in Aubrecht et al. (2008a) from layer 3 (the pink layer), layer 4 (the dark layer), and layer 5 (the white layer). Three samples (Fig. 4) were cut for inductively coupled plasma mass spectrometric (ICP-MS) analysis of trace elemental composition. Sample ICP-4 is of the clean white material from layer 5, ICP-5 is largely the dark material from layer 4, and ICP-3 includes some light and some dark layers from layers 5 and 6. Analyses were done by ActLabs Ontario. The detection limit for most elements is 0.1 ppm.

https://doi.org/10.1016/j.yqres.2010.03.005 Published online by Cambridge University Press

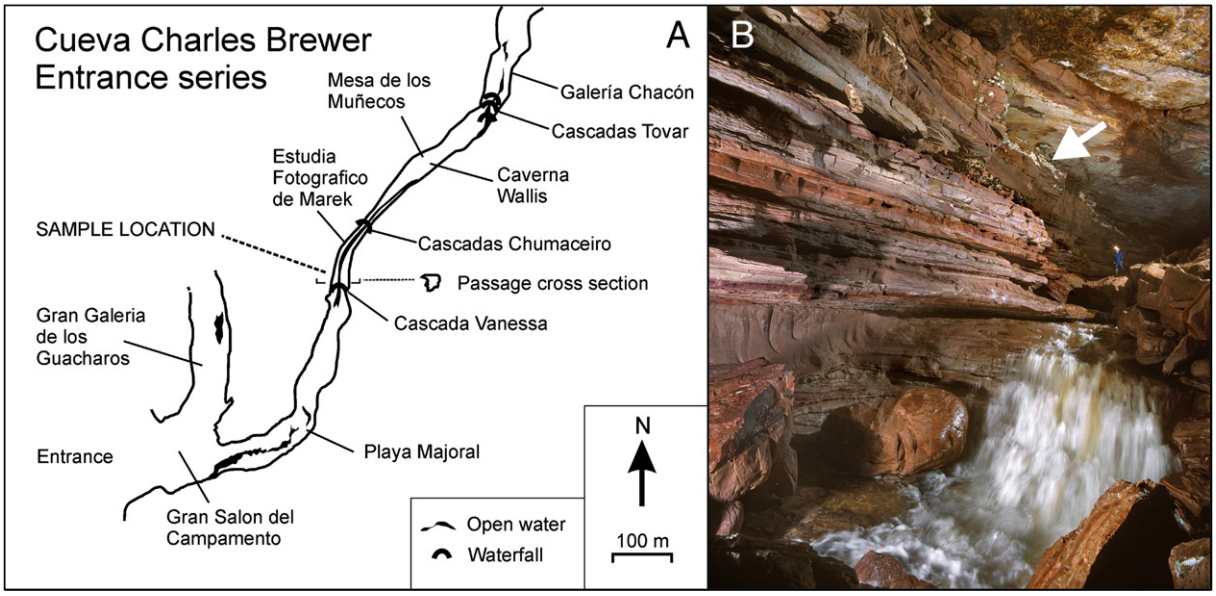

Figure 3. (A) Extract from survey of Cueva Charles Brewer (modified from Šmída et al., 2005) showing sample location in relation to the open water (solid black shapes) and the cascades (black semicircular symbols over the open water). (B) Photograph of Cascade Vanessa showing line of speleothems in wall above figure, marked with white arrow, some 8–12 m above water level, and above the highest flood level (photograph by Marek Audy, used by permission).

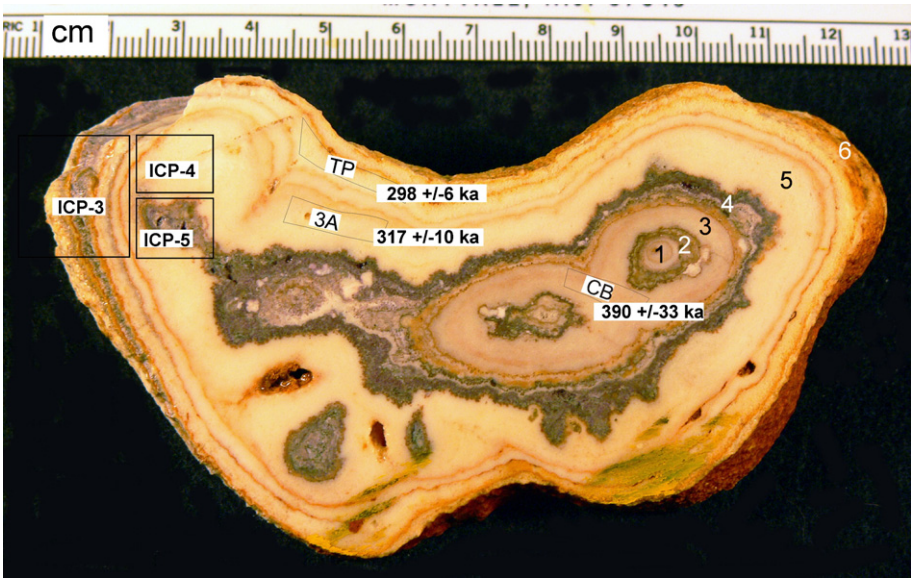

Figure 4. Sampled locations for TIMS dates (TP, 3A, CB) and for ICP analyses (ICP-3, ICP-4, ICP-5) and the stratigraphic layers (1 to 6). (The green marks at the base of the slice are artifacts from the saw.)

Results

Chronology

Isotopic data and ages are shown in Table 1. In Figure 5, the dates are plotted with the orbital eccentricity curve and with two marine isotope curves (the two are included because of the difference in dates of terminations IV and V) from Bassinot et al. (1994) and from Raymo and Ruddiman (2004).

The uranium concentration is low, at 30–110 ppb. The average 2σ error of $^{234}U/^{238}U$ is 0.18% and of $^{230}Th/^{234}U$ is 0.48% (instrumental reproducibility is 0.06% for $^{234}U/^{238}U$ and 0.11% for $^{230}Th/^{234}U$). The

Table 1
Isotopic data from TIMS analysis. Ratios are in activity ratios. Errors are 2 sigma. Age is quoted as the calculated age first and then the age adjusted for detrital contamination using initial $^{230}Th/^{232}Th$ values and error from typical crustal values. Decay constant values from Cheng et al. (2000) are $\lambda 230 = 9.1577 \times 10^{-6}$ year^{-1}, $\lambda 234 = 2.8263 \times 10^{-6}$ year^{-1}, $\lambda 238 = 1.55125 \times 10^{-10}$ year^{-1}.

Sample	From Edge (mm)	Age (ka)	Age (adj) (ka)	^{238}U conc. (μg/g)	^{232}Th conc. (μg/g)	$^{230}Th/^{234}U$ act. rat.	$^{234}U/^{238}U$ act. rat.	$^{230}Th/^{232}Th$ act. rat.	$^{234}U/^{238}U$ Initial
TP	4	301 +5 −4	298 +6 −6	0.11	0.06	1.127 ± 0.005	2.824 ± 0.003	16	5.271 ± 0.005
3A	11	324 +6 −6	317 +10 −10	0.03	0.03	1.127 ± 0.005	2.341 ± 0.005	8	4.351 ± 0.008
CB	21	408 +23 −19	390 +33 −31	0.10	0.10	1.051 ± 0.006	1.260 ± 0.003	4	1.825 ± 0.004

https://doi.org/10.1016/j.yqres.2010.03.005 Published online by Cambridge University Press

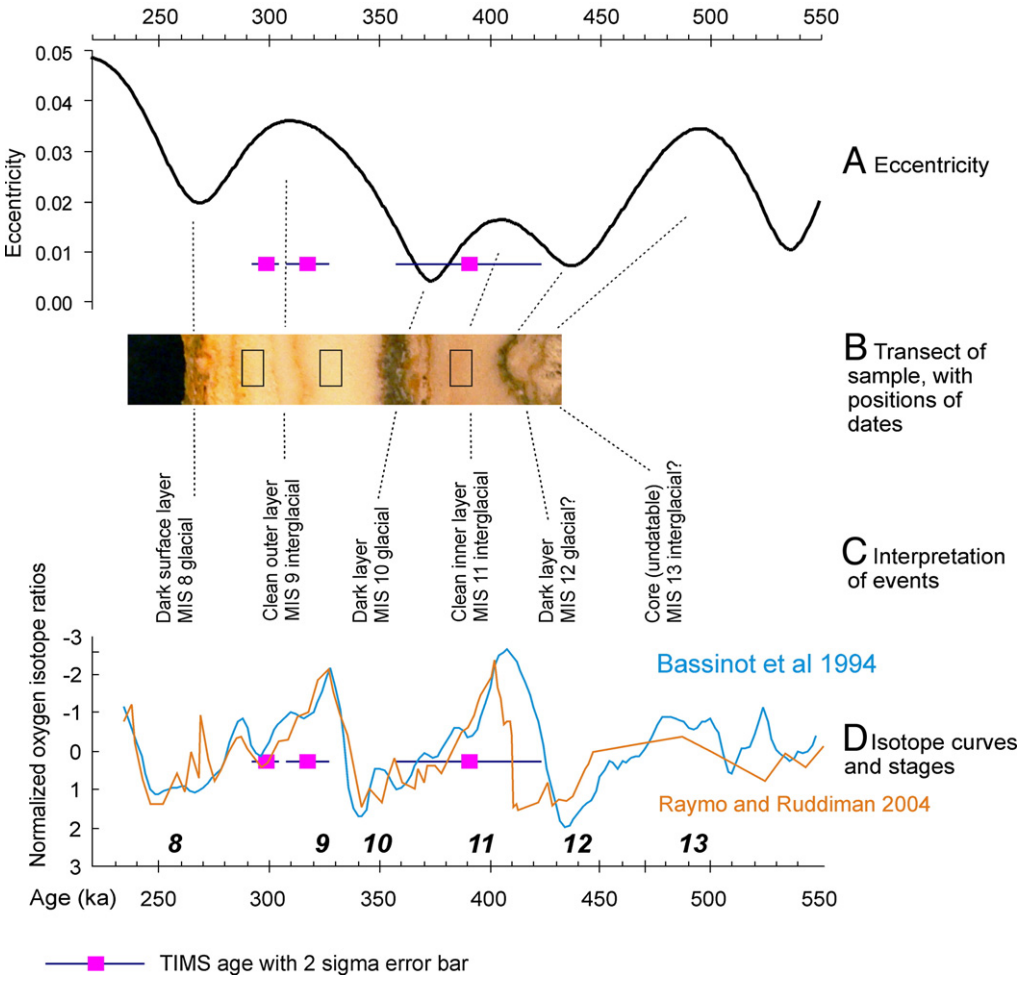

Figure 5. Dates shown in relation to (A) orbital eccentricity, (B) transect and position of dated horizons, (C) interpretation of events, and (D) marine isotopic curves from Bassinot et al. (1994) – blue line and text – and Raymo and Ruddiman (2004) – red line and text (the age model for this part of the curve is from Shackleton et al., 1990). The two marine curves are shown because estimates for the dates of isotope stage boundaries are somewhat variable here. The dotted lines highlight the most likely connections.

precision on the resultant dates varies with age; the 2σ precision on these middle to late Pleistocene dates is 2–8%. All dates are in stratigraphic order. The inner layer, at $390+33/-31$ ka, lies in Marine Isotope Stage (MIS) 11. The outer layer, with dates of 317 ± 10 ka and 298 ± 6 ka, lies in MIS 9. Growth rate is very low: the two dates in MIS 9 indicate a growth rate during the interglacial period of only 7 mm in 19,000 years or 0.37 ± 0.23 mm/ka. Using this growth rate, 4 mm represents 10.8 ± 6.7 ka, so this layer started to grow in 328 ± 12 ka and stopped in 287 ± 9 ka (shown by dotted lines in Fig. 5). Growth rate during the glacial periods was even lower—if we assume constant growth between samples 3A and CB, then the growth rate is 0.14 ± 0.06 mm/ka over the glacial period (obviously an overestimate since the interval includes some interglacial growth).

The initial $^{234}U/^{238}U$ ratios, at 1.8 to 5.3, are high and show a noticeable increase from the center outwards (triangle symbols in Fig. 6), anti-correlated with age.

The porous nature of this material initially gave cause for concern that, in spite of the low solubility of silica, the system may have been open for uranium migration (this would typically be indicated by either no significant differences between, or no stratigraphic coherence in, the ages). However, this coherent suite of dates suggests that the system has remained closed since deposition.

Composition (XRD and ICP-MS results)

The major mineral composition is quartz. XRD results from Aubrecht et al. (2008a) indicate that the white layer, layer 5, is predominantly Opal-A, with increasing proportions of micro-crystalline quartz in the inner layers.

Data on the trace elemental composition for elements of >1 ppm are shown in Table 2 (Appendix A). The major elements are shown graphically in Fig. 7: the more important elements are shown first (note that the scale is in ppt), and minor elements, second (scale in ppm). The dark layers are enriched in almost all elements compared with the white layer, especially in Fe and Al. The enrichment is 324% on average for all elements. Of the minor elements, the greatest proportional enrichment is for the heavy metals Ba, U, Ce, La, Nd, and Cr and least for the lighter metals B, Ca, Mg, Li, and Na.

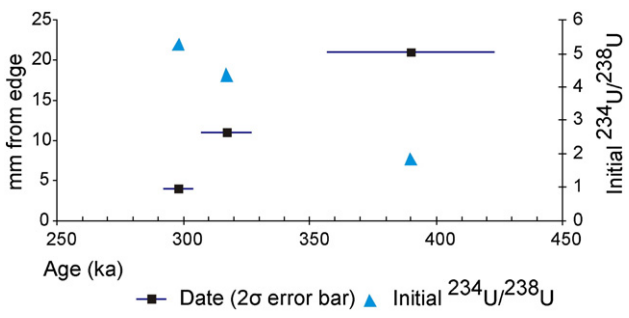

Figure 6. Dates and initial $^{234}U/^{238}U$ activity ratios.

https://doi.org/10.1016/j.yqres.2010.03.005 Published online by Cambridge University Press

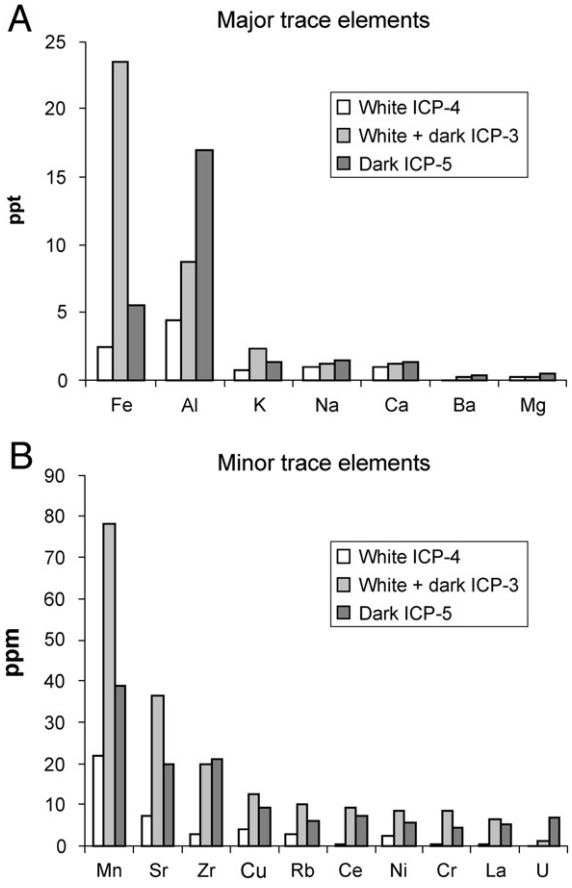

Figure 7. Trace element compositions of the three layers. "White ICP-4" is the pale peloidal outer layer 5, "White + dark ICP-3" includes some light and dark layers from 5 and 6, "Dark ICP-5" is the dark material from layer 4. Note the change in scale for the *y*-axis.

Discussion

Comparison with marine isotope curves (Fig. 5) suggests that the dated light-colored layers grew during the interglacial stages MIS 9 and 11. Thus the intervening dark-colored layers most likely correspond with the intervening glacial stages MIS 8, 10, and 12. These preliminary dates are too few to allow us, at this stage, to confidently correlate the properties and chronology of the layers with orbital parameters or with marine isotope stages. However, we can hypothesize, on the basis of typical controls on speleothem growth, that the faster lighter-colored growth is likely associated with warmer/wetter conditions and the slower darker-colored growth, with cooler/drier conditions. While these speleothems are not necessarily directly comparable with normal meteoric water speleothems, it is common for speleothems to grow more slowly in drier conditions. For example, Musgrove et al. (2001) showed that the fastest growth in a stalagmite from Texas is associated with greater moisture supply, and Vaks et al. (2003) used the timing of speleothem growth to reconstruct paleo-precipitation in Israel. It is also common for speleothems to show lower growth rates in cooler conditions: for example, Smith et al. (2006) used variations in speleothem growth rates to produce an extra-tropical, mean annual Northern Hemisphere temperature reconstruction for the past 500 years.

The limited research from this region suggests that glacial periods were indeed cooler. Rull (2004) notes that in the Neotropics, average temperature during the last glacial maximum (LGM) was probably some 8°C lower than today and 5°C lower in the Amazon lowlands. There is, as yet, no consensus about whether glacial to interglacial transitions in this region included significant changes in humidity. Schubert and Fritz (1985) and Pennington et al. (2000) suggest that it was significantly drier as well as cooler during glacial periods. The observation that the oldest peats found on the tepui tops are early to mid-Holocene in age, and the known requirement of wet conditions for peat formation does suggest that the tepui tops may have been arid or semi-arid before the early Holocene. However, Rull (2004 and 2005a) notes that a 40% reduction in precipitation on these very wet tepui summits (see Van der Hammen and Hooghiemstra, 2000) would have been relatively insignificant, that the tepui summits probably supported a cool and humid glacial period climate, and that the paucity of pre-Holocene peats may reflect paucity of studies rather than true absence.

If the generally slow growth rate of this sample is typical of other speleothems in the cave, then some of the larger samples may be considerably older than middle Pleistocene. If the observed association of this type of speleothem with waterfalls is causal, that is, if growth is triggered where a waterfall provides spray, then the locus of speleothem deposition should follow waterfall retreat and the oldest material should be found further downstream. An inference of this mode of development is that any one speleothem should have a life span limited by the rate of backcutting of the waterfall as well as by the rate of backcutting of the wall (many examples in this pristine cave can be seen of broken speleothems littering the floor amongst the collapsed rock). Speleothem growth will start as headward erosion brings the waterfall near, and, if the wall remains intact, growth will become limited and eventually halted as the waterfall continues to retreat and supply of spray is cut off.

Since the dates adjusted for detrital content are within error of the non-adjusted dates, it is apparent that detrital contamination is not significant in these old samples. However, for future research on younger material, isochron techniques may be required.

The increase in initial $^{234}U/^{238}U$ ratio over time suggests a change in the nature of the feeding liquid. Unlike normal speleothem feed water, this is not meteoric water dripping through overburden. Instead it is likely that the speleothems are fed by fine spray from the nearby waterfalls (Aubrecht et al., 2008a), a theory engendered by their apparent restriction within the cave to areas close to the waterfalls. The river water comes directly from the top of the tepui, so its chemistry will reflect conditions on the surface. The observed increase in supply of ^{234}U over time follows a very typical pattern consistent with radiogenic decay of ^{238}U in the host rock—this creates ^{234}U and the surface waters then become enriched in the slightly more soluble ^{234}U. An alternative source of feed water to the speleothems is the highly undersaturated moisture that condenses on the cave walls and rock surfaces (Lánczos et al., 2007; Aubrecht et al., 2008a). This rapidly dissolves silica, migrates to the speleothem surfaces by capillary action, and then concentrates by evaporation, depositing a layer on the speleothem surface. This water would equally pick up the more soluble radiogenically produced ^{234}U that accumulates over time in the host rock.

The elemental composition elucidates another facet of the picture. The dark material is consistently more concentrated in minor and trace elements than the pale material. Much of this is a simple reflection of the slower growth rate. If the surfaces collect dust or aerosol, then this material is more diluted by silica in the faster growing paler layers. Additionally, if deposition of silica is slow, the surface of the speleothem may have a thicker biological mat that can more effectively trap dust. However, the higher concentration may also reflect changing environmental conditions of humidity and weathering on the tepui surface. In conditions of reduced rainfall, the decreased runoff would become more concentrated in weathering- and soil-derived elements.

The proportions, as well as the concentrations, of trace elements vary between the light and the dark layers. The greater proportional enrichment of heavy metals compared to light metals may be a result of the biogenic mediation of deposition of the speleothems, organic chelation being known to favor heavy metals (Pitty, 1979: p.166-167). Alternatively it may be the result of increased concentrations or changing proportions of humic and fulvic materials in the soils. Humic

https://doi.org/10.1016/j.yqres.2010.03.005 Published online by Cambridge University Press

substances in the water will chelate heavy metals and fulvic materials are even more effective: Fe, Al, Cu are particularly efficiently chelated by fulvics especially in acidic solutions (Pitty, 1979). Baker et al. (1998) showed that the proportions of humics and fluvics vary with climatic conditions in calcite speleothems—it would not be surprising if this were also true of silica speleothems.

Conclusion

The first suite of U–Th dates from a silica speleothem is presented here. These are from the extraordinary biospeleothems of the large sandstone cave, Cueva Charles Brewer, of Churi-tepui, Chimantá Plateau, SE Venezuela. Mineralogically, the sample is Opal-A with increasing micro-quartz towards the core. The sample grew in alternating narrower dark-colored and wider light-colored layers. Results from elemental study of both layers and dating of the light-colored bands suggest that:

- the uranium concentration is low, at 30–110 ppb, but not too low to preclude effective dating;
- the high ^{232}Th concentrations (indicating significant detrital contamination) are not problematic for these old samples, but future dating of younger material may require isochron techniques;
- the inner layer, dated at $390+33/-31$ ka, grew during MIS 11, and the outer layer, dated at 317 ± 10 ka and 298 ± 6 ka, grew during MIS 9;
- initial ^{234}U/^{238}U ratios are high, at 1.8 to 5.3, and increase over time as radiogenic production of more soluble ^{234}U in the host rock proceeds;
- the growth rate is very low, the fastest being 0.37 ± 0.23 mm/ka during the interglacial period of MIS 9 and the slowest during the MIS 10 glacial period, at a maximum rate of 0.14 ± 0.06 mm/ka;
- the slow growth rate suggests that other, larger, samples from this cave may be considerably older than mid-Pleistocene;
- the dark layers are enriched in almost all elements compared with the lighter layers, with the greatest proportional enrichment for heavy metals, reflecting the slower growth and perhaps reduced rainfall during glacial periods;
- the pattern in this sample suggests an association of more rapid, paler colored growth with interglacial periods (MIS 9 and 11) and slower, dark-colored growth with glacial periods (MIS 8, 10, and 12).

These preliminary data are the basis for the hypothesis that the growth, color, and elemental composition of these silica layers correlate with wet–dry cycles (that also correlate broadly with glacial–interglacial cycles). The implication is that these silica speleothems, like their calcitic counterparts, probably contain a record of paleoenvironmental change.

Although this report only includes the first dates on these speleothems, it bodes very well for continued studies. Larger speleothems will likely have a longer record, and younger speleothems will fill in the gaps. The growth rate and habit are valuable in themselves as indicators of changing conditions, but the more exciting possibility that this research opens up is the potential that these speleothems will also house a useful isotopic record. The reconstruction of the sedimentary sequence of this sample is the first step in a reconstruction of Quaternary palaeoenvironmental conditions for the region. Paleoclimatic proxies for this region are rare and short (e.g., Curtis et al., 1999, have only 12.6 ka of record; for Rull, 2005a, only 6 ka)—the possibility of a paleoenvironmental record that stretches back half a million years is enticing.

The cave is located close to the southernmost limit of the intertropical convergence zone (ITCZ) in July. Thus, the area is potentially highly sensitive to variations in the strength and location of the July ITCZ, which will impact regional precipitation and the regional forest–savanna boundary. These effects have been recognized in stable carbon isotope profiles from latest Pleistocene–Holocene soils in the northernmost Brazilian Amazon (Desjardins et al., 1996), but the precise effects of humid–arid cycles on the tepui summit ecosystems are unknown and details from the earlier Pleistocene are unknown. The absence of tepui-summit peats older than early Holocene has been interpreted to indicate that peat accumulation may occur only in high-precipitation, interglacial situations (Shubert et al., 1994). If this is correct, a significant glacial–interglacial shift in carbon stable isotope systematics and also trace element mobilization of speleothem feed water can be expected. A high-resolution δ^{13}C and trace element record from the Cueva Charles Brewer speleothems can therefore be expected to illuminate ~500,000 years of precipitation regime shift in the northern Amazon forest–savanna ecotone. Future research will focus on higher resolution dating, minimization of errors, and high-resolution isotopic and trace element studies.

In 2005, Rull (2005b) stated that "environments… [of] the highest tepui summits during the LGM and other glacial phases are unknown." Hopefully, by extending the present work, we may be able to finally understand the localized effects of glacial episodes on these unique environments. In addition, we may be able to document the extent of Holocene anthropogenic impacts, since the cave is now only a few kilometers from the modern, anthropogenically mediated forest–savanna boundary.

Acknowledgments

The Muchimuk 2009 expedition was mounted under the auspices of the Sociedad Venezolana de Ciencias Naturales. Financing and support was provided by Fundacion EXPLORA and in part by an NSERC grant to J.L. This is Ottawa-Carleton Geoscience Centre, Isotope Geochemistry and Geochronology Research Facility contribution No. 52. Thanks to referees and editors for their very helpful comments.

Appendix A

Trace elemental composition from ICP-MS analysis. Values are in ppm. Elements below 1 ppm (Cd, Hf, Er, Be, Ho, Ag, Cs, Eu, Bi, Se, Zs, Nb, Mo, In, Sn, Sb, Te, Pr, Sm, Gd, Tb, Dy, Ge, Tm, Lu, Ta, W, Re, Ti) are not included in the table.

Analyte Symbol	ICP-4 White Material (ppm)	ICP-3 White + dark Material (ppm)	ICP-5 Dark Material (ppm)
Al	4500	8800	17,000
Fe	2500	23500	5500
Ca	1000	1200	1300
Na	950	1250	1500
K	800	2300	1300
Mg	300	300	500
Mn	22	78	39
Ba	13	311	364
Sr	7.5	36.7	20
B	5	2	< 1
Cu	4.3	12.5	9.3
Zn	3.1	4.1	8.2
Rb	3	10.1	6
Zr	3	20	21
Ni	2.7	8.6	5.8
Li	1.5	1.1	3
As	1.4	2.9	1.9
V	< 1	3	2
Cr	0.7	8.5	4.6
Ga	0.7	2.6	2.1
Ce	0.7	9.6	7.2
La	0.5	6.7	5.2
Pb	0.5	3	2
Y	0.4	2.1	4.3
Nd	0.4	3.8	5.7
Th	0.2	1.3	1.6
U	0.2	1.2	6.8
Total	1.0e + 4	3.8e + 4	2.8e + 4

References

Aubrecht, R., Brewer-Carías, C., Šmída, B., Audy, M., Kováčik, L., 2008a. Anatomy of biologically mediated opal speleothems in the world's largest sandstone cave: Cueva Charles Brewer, Chimantá Plateau, Venezuela. Sed. Geol. 203, 181–195.

https://doi.org/10.1016/j.yqres.2010.03.005 Published online by Cambridge University Press

Aubrecht, R., Lánczos, T., Šmída, B., Brewer-Carías, C., Mayoral, F., Schlögl, J., Audy, M., Vlcek, L., Gregor, M., 2008b. Venezuelan sandstone caves: a new view on their genesis, hydrogeology and speleothems. Geologia Croatica 61 (2–3), 345–362.
Baker, A., Genty, D., Smart, P.L., 1998. High resolution records of soil humification and paleoclimate change from variations in speleothem luminescence excitation and emission wavelengths. Geology 26, 903–906.
Bassinot, F.C., Labeyrie, L.D., Vincent, E., Quidelleur, X., Shackleton, N.J., Lancelot, Y., 1994. The astronomical theory of climate and the age of the Brunhes-Matuyama magnetic reversal. Earth Planet. Sci. Lett. 126, 91–108.
Brewer-Carías, C., 2005. Las Espeleotemas de la Cueva Charles Brewer. In: Michelangeli, Armando (Ed.), Tepuy, Colosos de la Tierra, pp. 310–327. Fundación Terramar, Altolitho, Caracas. 344 pp.
Briceño, H.O., Schubert, C., 1990. Geomorphology of the Gran Sabana, Guayana Shield, southeastern Venezuela. Geomorphology 3, 125–141.
Burne, R.V., Moore, L.S., 1987. Microbialites: organosedimentary deposits of benthic microbial communities. Palaios 2, 241–254.
Chacón, A., Mesa, J., Mayoral, F., 2006. La Cueva Charles Brewer. Revista FACES, Caracas 3 (13), 28–53.
Cheng, H., Edwards, R.L., Hoff, J., Gallup, C.D., Richards, D.A., Asmerom, Y., 2000. The half-lives of uranium-234 and thorium-230. Chem. Geol. 169, 17–33.
Cruz Jr., F.W., Burns, S.J., Karmann, I., Sharp, W.D., Vulle, M., Cardaso, A.O., Ferrari, J.A., Dias, P.L.S., Vlana Jr., O., 2005. Insolation-driven changes in atmospheric circulation over the past 116,000 years in subtropical Brazil. Nature 434, 63–65.
Curtis, J.H., Brenner, M., Hodell, D.A., 1999. Climate change in the Lake Valencia Basin, Venezuela, 12600 yr BP to present. Holocene 9, 609–619.
Desjardins, T., Carneiro Filho, A., Mariotti, A., Chauvel, A., Girardin, C., 1996. Changes in the forest-savanna boundary in Brazilian Amazonia during the Holocene revealed by stable isotopes of soil organic carbon. Oecologia 108, 749–756.
Edmond, J.M., Palmer, M.R., Measures, C.I., Grant, B., Stallard, R.F., 1995. The fluvial geochemistry and denudation rate of the Guayana Shield in Venezuela, Colombia, and Brazil. Geochim. Cosmochim. Acta 59, 3301–3325.
Gibbs, A.K., Barron, C.N., 1993. The geology of the Guyana Shield. Oxford, Clarendon Press. 245pp.
Hill, C.A., Forti, P., 1997. Cave minerals of the world. National Speleological Society, Huntsville, Alabama. 238pp.
Ivanovich, M., Latham, A.G., Ku, T.-l., 1992. Uranium-series disequilibrium applications in geochronology. In: Ivanovich, M., Harmon, R.S. (Eds.), Uranium-series Disequilibrium: Applications to Earth, Marine and Environmental Sciences, 2nd edition. Clarendon Press, Oxford, pp. 62–89.
Lánczos, T., Aubrecht, R., Schlögl, J., Šmída, B., Brewer-Carías, C., 2007. Preliminary results of the Tepuy 2007 expedition to the Venezuelan table mountains—water geochemistry and its relation to the genesis of the quartzite karst. In: Fl'aková, R., Šenišová, Z. (Eds.), Proceedings of the Hydrogeochémia 2007 conference, 7th–8th June 2007, Bratislava. Slovak Association of Hydrogeologists, Bratislava, pp. 136–141.
Musgrove, M., Banner, J.L., Mack, L.E., Combs, D.M., James, E.W., Cheng, H., 2001. Geochronology of late Pleistocene to Holocene speleothems from central Texas; implications for regional paleoclimate. Bull. Geol. Soc. Am. 113, 1532–1543.
Pennington, R.T., Credo, D.E., Pendry, C.A., 2000. Neotropical seasonally dry forests and Quaternary vegetation changes. J. Biogeogr. 27, 261–273.
Piccini, L., Mecchia, M., 2009. Solution weathering rate and origin of karst landforms and caves in the quartzite of Auyan-tepui (Gran Sabana, Venezuela). Geomorphology 106, 15–25.
Pitty, A.F., 1979. Geography and soil properties. American Geographical Society. 287.
Potter, P.E., 1997. The Mesozoic and Cenozoic drainage of South America: a natural history. J. S. Am. Earth Sci. 10, 331–344.
Raymo, M.E., Ruddiman, W.F., 2004. DSDP Site 607 Isotope Data and Age Models, Data Contribution Series #2004-010. NOAA/NGDC Paleoclimatology Program, Boulder, CO, USA.
Rull, V., 2004. Biogeography of the 'Lost World': a palaeoecological perspective. Earth-Sci. Rev. 67, 125–137.
Rull, V., 2005a. Vegetation and environmental constancy in the Neotropical Guayana Highlands during the last 6000 years? Rev. Palaeobot. Palynol. 135, 205–222.
Rull, V., 2005b. Biotic diversification in the Guyana Highlands: a proposal. J. Biogeogr. 32, 921–927.
Santos, J.O.S., Potter, P.E., Reis, N.J., Hartmann, L.A., Fletcher, I.R., McNaughton, N.J., 2003. Age, source, and regional stratigraphy of the Roraima Supergroup and Roraima-like outliers in northern South America based on U–Pb geochronology. Geol. Soc. Am. Bull. 115, 331–348.
Schubert, C., Fritz, P., 1985. Radiocarbon ages of peat, Guayana Highlands (Venezuela). Naturwissenschaften 72, 427–429.
Šmída, B., Audy, M., Mayoral, F., 2005. Cueva Charles Brewer: largest quartzite cave in the world. NSS News, pp. 13–31. January 2005.
Smith, C.L., Baker, A., Fairchild, I.J., Frisia, S., Borsato, A., 2006. Reconstructing hemispheric-scale climates from multiple stalagmite records. Int. J. Climatol. 26, 1417–1424.
Shackleton, N.J., Berger, A., Peltier, W.R., 1990. An alternative astronomical calibration of the lower Pleistocene timescale based on ODP Site 677. Trans. R. Soc. Edinburgh, Earth Sci. 81, 251–261.
Shubert, C., Fritz, P., Aravena, R., 1994. Late quaternary paleoenvironmental studies in the Gran Sabana (Venezuelan Guyana Shield). Quatern. Int. 21, 81–90.
Twidale, C.R., Romani, J.R.V., 2005. Landforms and geology of granite terrains. Taylor and Francis. 351.
Urbani, F., Compère, P., Willems, L., 2005. Opal-a Speleothems of Wei-Assipu-Tepui, Roraima Province, Brazil. Boletín de la Sociedad Venezolana de Espeleología 39, 21–26.
Vaks, A., Bar-Matthews, M., Ayalon, A., Schilman, B., Gilmour, M., Hawkesworth, C.J., Frumkin, A., Karufam, A., Matthews, A., 2003. Paleoclimate reconstruction based on the timing of speleothem growth and oxygen and carbon isotope composition in a cave located in the rain shadow in Israel. Quatern. Res. 59, 182–193.
Van der Hammen, T., Hooghiemstra, H., 2000. Neogene and Quaternary history of vegetation, climate and plant diversity in Amazonia. Quatern. Sci. Rev. 19, 725–742.
Willems, L., Compere, P., Hatert, F., Puclet, A., Vicat, J.P., Ek, C., Boulvain, F., 2002. Karst in granitic rocks, South Cameron: cave genesis and silica and taranakite speleothems. Terra Nova 14, 355–362.
White, W.B., Jefferson, G.L., Haman, J.F., 1967. Quartzite karst in Southeastern Venezuela. Int. J. Speleol. 2, 309–314.
Wray, R.A.L., 1999. Opal and chalcedony speleothems on quartz sandstones in the Sydney region, southeastern Australia. Aust. J. Earth Sci. 46, 623–632.